Wake vortex gliding

Pavel Zikmund
Brno University of Technology
Technická 2, Brno, 616 69, Czech Republic

Abstract

Airplanes and birds can save energy by flying in formation. The energy is harvested from the wake vortex of the formation leader. This paper brings flight performance feasibility study of an extreme formation when a big airliner is followed by a small UAV. Models of B 747 wake vertices are laid out and parameters of the UAV designed for flight in the wake vortex are introduced. Regions with sufficient energy for gliding flight are analysed for different vortex models.

Nomenclature

a_1	Squire's parameter
b	Span, m
r	Radial dimension, m
r_c	Vortex core radius, m
t	Time, s
t'	Reference time = $2\pi b^2\Gamma^{-1}$, s
V_t	Induced tangential velocity, ms^{-1}
α	Oseen parameter = 1.2564
δ	Eddy viscosity coefficient
Γ	Vortex circulation, m^2s^{-1}
ν	Kinematic viscosity, m^2s^{-1}

1. Introduction

Cruise flight in transonic speed requires powerful engines. The mentioned statement is going to be broken by a wake vortex gliding idea. Airliners produce a vast of energy to fly fast. Part of the energy is consumed by friction, pressure and wave drag. The last drag component is induced drag. Energy consumed to overpower the induced drag does not vanish immediately. It is transformed to strong wake vertices pair shed behind airliner. These vertices decay very slowly. Airplanes and birds flying in formation use the vortex energy to decrease required power of the followers. Is it possible to achieve 100 % of energy savings in case of a big airliner followed by a small UAV? The paper tries to answer this question.

Wake vertices have been studied intensively since big airliners began to fly. That is caused by its dangerous consequences for other airplane vortex encounter. Some airplane accidents stimulated researchers to analyse wake vortex behaviour [1]. Wind tunnel experiments and in-flight tests by NASA [2, 3, 4] were carried out. Upward induced speeds within vortex core reach astonishing values over 10 % of forward speed.

Flying in formation was discovered by migrating bird flocks. Birds use V shape or line formation to save energy during long flights. The same advantage was measured by real airplanes [5]. Savings of 14 % of fuel was measured in the second airplane in close formation in cruise regime. The same energy savings was estimated also for birds [6]. Induced velocities in wake allow them flap with slower frequency and extend the gliding phase of flight. The wake vortex gliding idea is extreme example of formation flight. A span of UAV glider is smaller than airliner's wake vortex core radius. The UAV is supposed to fly in region with maximum upwards induced velocities. The idea concept was published in 2013 [7].

This paper begins by literature search and case study definition of wake vortex models. Following chapter summarize design process of the UAV suitable for flight in wake vertices. The basic parameters and drag polar of the UAV are specified. Analysis of gliding in wake vortex brings analytical results supported by CFD validation. Discussion and conclusion complete the paper.

Copyright © 2015 by Pavel Zikmund. Published by the EUCASS association with permission.

2. Vortex models

Models of wake vertices are simulated as fully developed. The first stage of vortex life when vortex is formed is not solved. Ambient atmosphere is considered without any significant turbulence. The airliner B747 was chosen as wake vortex generating airplane for the case study. The atmosphere state is defined by international standard atmosphere conditions in typical B747 cruise altitude 10 668 m. The forward speed is 0.85 M which means 252 ms^{-1} in given conditions. The following UAV air speed is calculated from forward and upward speed components of the wake vortex. The Airliner with estimated weight $327x10^6$ kg creates a wake vortex pair with initial circulation $\Gamma_0 = 660$ m^2s^{-1}. Iversen, Lamb-Oseen and Hallock-Burnham models were used in the vortex gliding idea analysis. Iversen's model [8] belongs among the first wake vortex descriptions which give good matching to experiments. Induced velocity distribution and vortex decay is given by dimensionless graphs in figure 1.

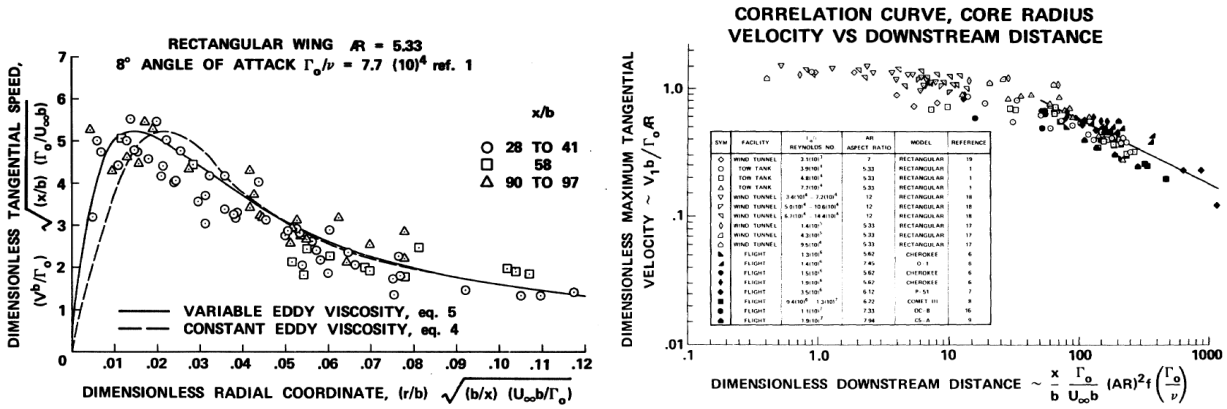

Figure 1: Induced velocity distribution and decay of Iversen model [8]

Lamb-Oseen and Hallock-Burnham induced velocity models [9] depends strongly on a vortex core size. The vortex Models are defined by the following equations for Lamb-Oseen (1) and Hallock-Burnham (2).

$$V_t(r) = \frac{\Gamma_0}{2\pi r}\left[1 - e^{-\alpha\left(\frac{r}{r_c}\right)^2}\right] \quad (1)$$

$$V_t(r) = \frac{\Gamma_0}{2\pi r}\frac{r^2}{r^2 + r_c^2} \quad (2)$$

2.1 Vertices initial size and growth

Iversen vortex model decay was obtained from dimensionless maximum tangential velocity in figure 1. The two other vortex models decay is given by vortex core radius growth. The first stage of vortex life is characterized by very small circulation decrease. Therefore vortex circulation is considered as a constant in the range of $t < t'$ [10, 11]. Tangential induced velocity decreases in spite of constant value of circulation. That is given by growing of a vortex core radius. Size of vortex core radius differs in literature within the range of 1 to 7 % of airplane span [12]. The initial core size and growth rate was obtained from literature [9, 13]. The initial value of 1 % of span was used. The core grow describe the following equation (3).

$$r_c = \sqrt{r_{c0}^2 + 4\alpha\delta\nu t} \quad (3)$$

Where eddy viscosity coefficient δ is given by (4)

$$\delta = 1 + a_1 Re = 1 + a_1 \frac{\Gamma}{\nu} \quad (4)$$

Value $5x10^{-5}$ of Squire's parameter a_1 was estimated with respect to literature [9]. The time history of maximal upwards induced velocities is showed in figure 2. The figure also shows comparison of induced velocity distribution of all three vertices models in distance 15 s from vortex generating airplane.

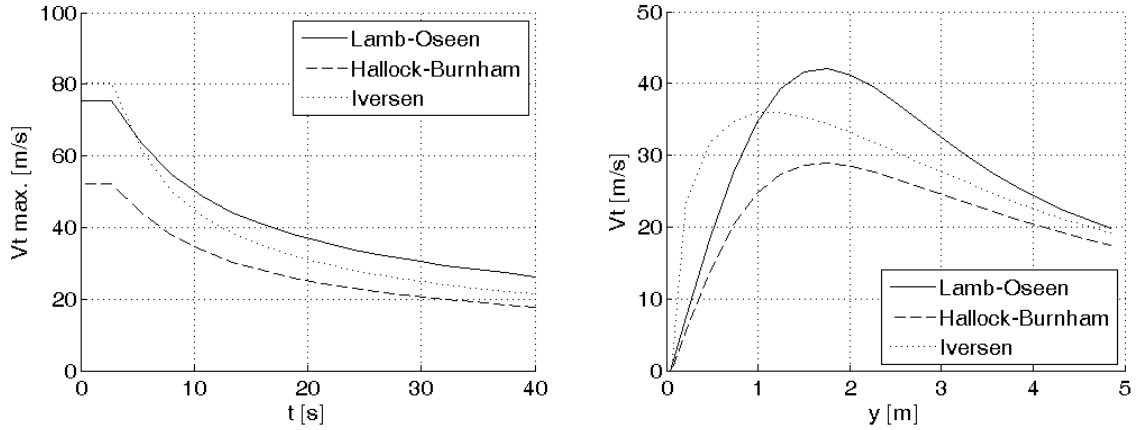

Figure 2: Vertices models comparison, time history and radial distribution of tangential velocities

3. UAV preliminary design

Detailed description of the UAV preliminary design is out of the paper focus. Master thesis [14] gives deeper insight to the design than this chapter which brings only brief process characterization and results. The goals of the design were geometry of UAV and polar estimation. The inputs to design process were vortex characteristics and the airliner cruise regime parameters. These pre-requisites are defined in previous chapter about wake vortex models. Geometrical design and drag polar estimation were carried out iteratively to achieve satisfactory results. Roskam method [15] was used for drag polar estimation.

Wing loading value is a surprising parameter which was obtained from the preliminary design. The ratio of the UAV weight and wing area reaches value 500 kgm^{-2} which is comparable to the airliners wing loading. The fuselage is shaped due to Whitcomb's area rule [16] to eliminate wave drag in transonic flight. Figure 3 shows preliminary sketch of the UAV.

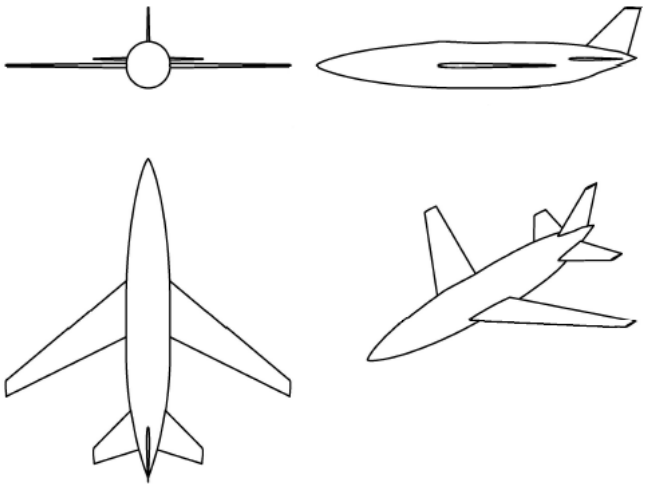

Figure 3: UAV concept layout [14]

Control surfaces are designed in the following configuration. The ailerons are going to be supported by spoilers [17]. The tail surfaces are all moving. Main characteristics of the UAV are presented in the following table 1.

Table 1: UAV basic characteristics

Weight	160 kg	Wing span	1.45 m
Wing area	0.32 m^2	Length	1.6 m

The drag polar is estimated in the following form (5).

$$c_D = c_{D0w} + c_{D0fus} + c_{D0emp} + c_{DL} \cdot c_L^2 + c_{Dtrans} + c_{Dctrl} \quad \textbf{(5)}$$

The first three coefficients represent wing, fuselage and empennage drag in zero lift condition. The next multiplied variables mean induced drag. The coefficient c_{Dtrans} represents wave drag in transonic speed. The last coefficient covers drag due to necessary control surfaces deflection. This value was estimated from the literature [14, 17]. The following Table 2 shows the comparison of the mentioned coefficients. The induced drag is considered in the cruise regime which is characterised by lift coefficient value 0.418.

Table 2: Drag coefficient estimation

	Variable	**Value [-]**	**Value [%]**
Wing zero lift drag	c_{D0w}	0.0044	10.8
Fuselage zero lift drag	c_{D0fus}	0.0129	31.7
Tail unit drag	c_{Demp}	0.0022	5.4
Induced drag	$c_{DL}\ c_L^{\ 2}$	0.0137	33.7
Wave drag	c_{Dtrans}	0.0025	6.1
Control surfaces drag	c_{Dctrl}	0.0050	12.3
Total drag	c_D	0.0407	100.0

4. Gliding feasibility analysis

Is it possible to achieve 100 % of energy savings in a cruise flight? This question from the introduction can be answered now. The necessary pre-requisites the wake vertices models and the UAV drag polar were defined in foregoing chapters. A simple condition has to be fulfilled to answer the question positively. UAV's gliding ratio has to be higher than available glide ratio. The available gliding ratio is given by wake vortices models. Upwards induced and forward velocities ratio specifies values of gliding ratio distribution. UAV's gliding ratio comes from UAV's drag polar. In case that UAV's gliding ratio is higher than available can the UAV keep at least the same speed as the airliner. The value of UAV's glide ratio is 10.3 from the drag polar in a cruise regime. Available gliding ratio values are shown in figures 4 – 6. Dark red colour belongs to area where the induced velocities are not enough strong. Dark blue denotes the side of vortex when induced velocities aim downwards. Colourful area maps the region where the UAV can harvest enough energy to follow the airliner.

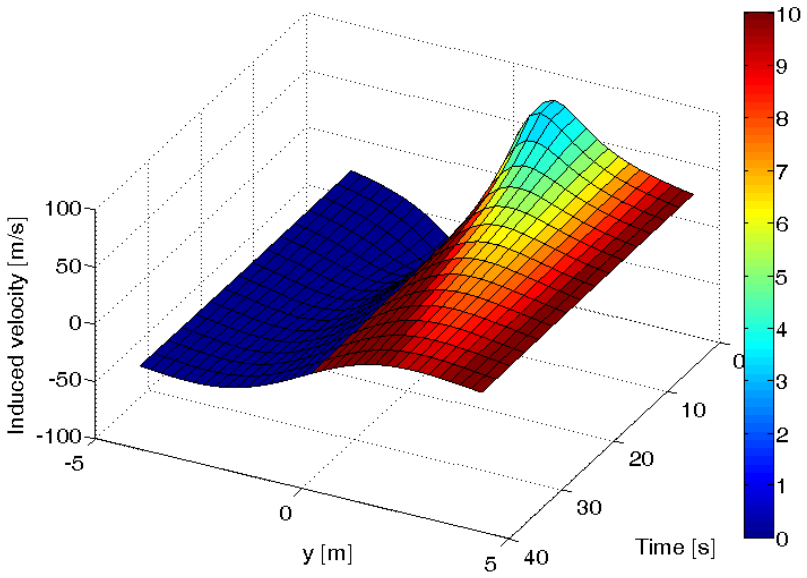

Figure 4: Available gliding ratio (in colour scale) for Lamb-Oseen vortex model

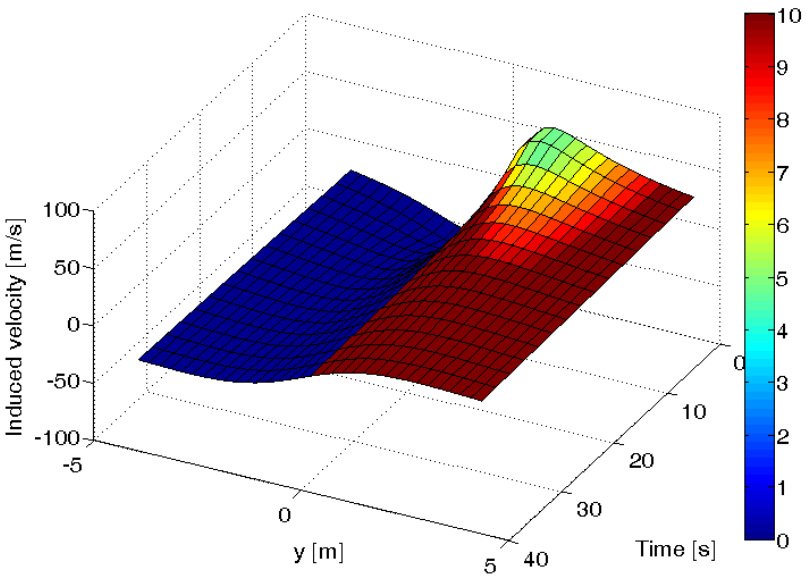

Figure 5: Available gliding ratio (in colour scale) for Hallock-Burnham vortex model

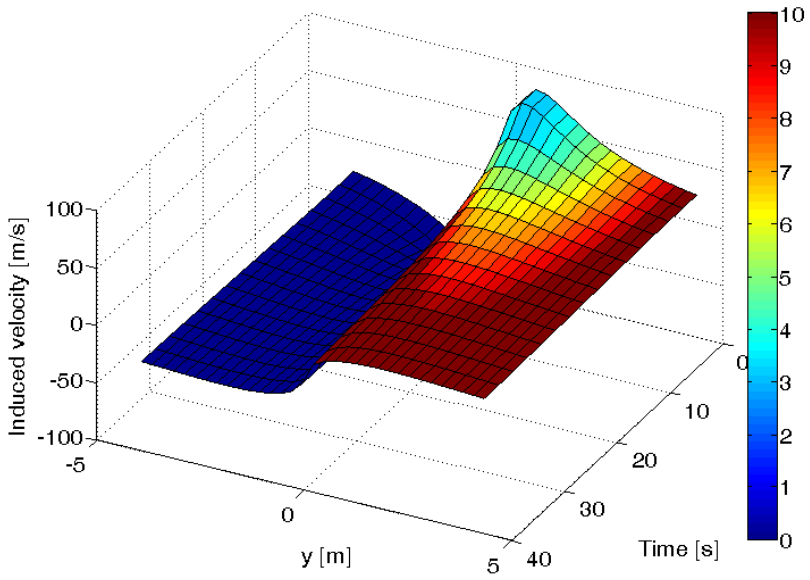

Figure 6: Available gliding ratio (in colour scale) for Iversen vortex model

4.1 CFD drag polar validation

Drag polar estimation by Roskam method [15] does not comprise the fact of flying in vortex. Therefore, estimated drag polar was validated by a CFD analysis. Only the wing was simulated in a vortex because of limited computer performance. The vortex influence was considered to be the most significant on the wing. Hallock-Burnham vortex model was applied in the analysis. ANSYS Fluent Release Version 14.5 was used.

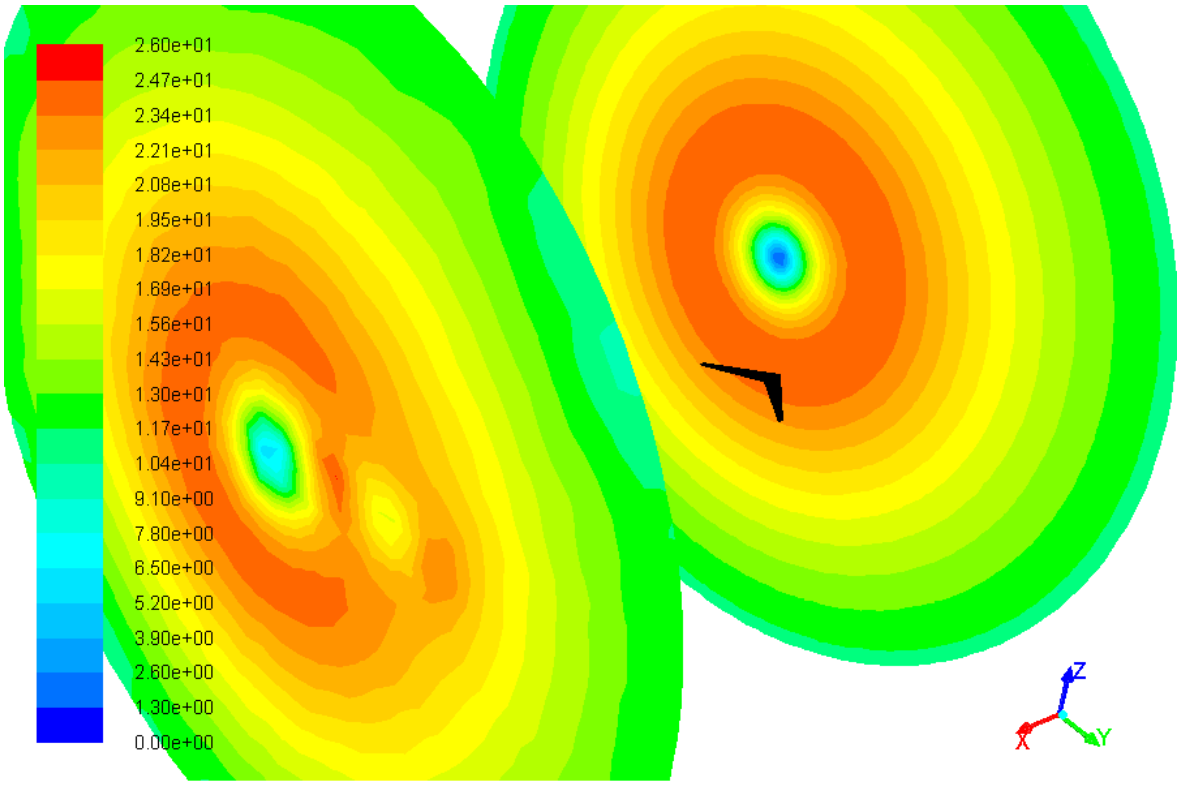

Figure 7: Tangential velocity (ms^{-1}) contours in inlet and outlet of cylindrical computational domain, t = 15 s

Density-based implicit solution was setup and viscous Spalart-Allmaras turbulence model was used in the CFD simulation. The wake vortex was defined by user defined function as a tangential velocity distribution on the inlet side of cylindrical computational domain. Mirror boundary condition was prescribed for lateral area of the cylinder. The domain consisted of 2.1×10^6 cells. Figure 7 shows the wing position in the domain and tangential velocity distribution on inlet and outlet bases. Some cases were analysed with different position in the wake vortex. The angle of attack was adjusted to get lift force corresponding to the cruise flight.

Drag and lift force directions cannot be found out simply. The incoming velocity direction varies along the whole domain. Therefore, the coefficient c_x was determined instead of c_D. Positive x axis direction is defined in figure 7. Coefficient c_x includes x direction component of drag and also lift component acting in opposite direction. The drag components of the rest of the airplane are added to the c_x of the wing obtained from CFD. Figure 8 shows resultant x direction force coefficient of the whole UAV. Two cases of wake vortex strength were defined by the distance 10 and 15 s from the airliner. Figure 8 indicates that the distance of 15 s is near the breaking point between areas where the UAV can and cannot glide.

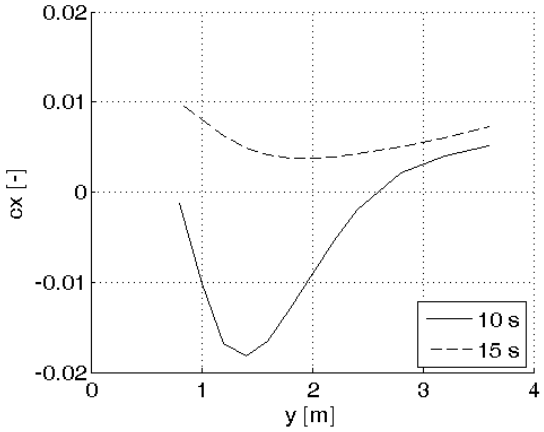

Figure 8: x direction force coefficient of gliding UAV in Hallock-Burnham vortex model. The results are plotted in dependence on distance from vortex core and for 10 and 15 s vortex life time.

CFD gives more pessimistic results than analytical analysis. The x direction force acting on UAV has positive value in case of 15 s distance behind the airliner. It means that UAV can't fly with required speed. Results obtained for the distance of 10 s offer nearly 2 m wide area where the c_x is negative. The UAV is pushed forward and even has drag reserve. This reserve can be consumed to generate electrical energy required to control and other UAV's systems.

5. Discussion

Results of gliding feasibility study give encouraging results. The wake vertices defined in the paper contain enough energy to push the UAV in cruise speed of the airliner. The wake vortex gliding concept has some inconsistent points on the other side. Gliding in transonic speed is physically possible but it is paid by extreme UAV's parameters. The weight of 160 kg and wing area 0.32 m^2 lead to very heavy structure. Fuselage size is limited by drag polar. Unbalanced ratio of wing and fuselage size would lead to insufficient glide ratio. Therefore, heavy structure is only the solution. The average density of designed UAV structure is approximately 3 500 kgm^{-3}. The negative consequence is stall speed about 320 km/h for plain wing without any flaps in condition of zero altitude of international standard atmosphere.

Vortex models are another controversy. Used vortices models were validated by flight measurement in calm atmosphere condition. Turbulent air cause faster wake vertices decay than a calm atmosphere.

Controllability in the vortex is the last unknown. What happens when the UAV approach the vortex axis where induced speed gradient reaches maximal value? The controllability analysis needs to be done to answer the question.

6. Conclusions

The presented work brought feasibility study of the wake vortex gliding idea. Three vertices models were chosen to describe B747 airliner's wake vortex in the cruise regime. The next steps were design of the UAV and its drag polar estimation. Basic parameters and drag polar estimation are introduced in the paper without detailed study. These results were used to establish regions with sufficient upwards induced velocity. The last part of the analysis is CFD validation of analytical drag polar estimation. The wing in wake vortex was simulated because analytical drag polar estimation does not comprise the influence of wake vortex.

The analysis identified region in wake vortex of B747 where the gliding flight of the UAV in transonic speed is possible. The UAV designed for this purpose has extreme value of the wing loading. Weight of 160 kg and wing area of 0.32 m^2 require heavy structure of the UAV. The paper proved that gliding in wake vertices of big airliners is possible but controllability analysis has to be done to confirm this conclusion.

Acknowledgement:

The work leading to these results was supported by Czech Science Foundation in the frame of GP14-16370P project "Wake vortex gliding as a new propulsion concept for Unmanned Aerial Vehicles".

References

[1] Bruin, A. 2000. Wake vortex evolution and Encounter (WAVENC). Air & Space Europe. 84-87.
[2] Rossow, V. 1999. Lift-generated vortex wakes of subsonic transport aircraft. *Progress in Aerospace Science*, 35.6: 507-660.
[3] Vicroy, D. D. 1998. Recent NASA wake-vortex flight tests, flow-physics database and wake-development analysis. SAE transactions, 107: 1764-1777.
[4] Garodz, L. J. et al. 1974. The Measurement of the Boeing 747 Trailing Vortex System Using the Tower Fly-by Technique, FAA-RD-73-156. National Aviation Facilities Experiment Center.
[5] Ray, R. J. 1998. Flight test techniques used to evaluate performance benefits during formation flight. In *NASA Conference publication*. NASA.
[6] Weimerskirch, H. et al. 2001. Energy saving in flight formation. *Nature*, 413.6857: 697-698.
[7] Zikmund, P., Popela, R. 2013. Wake vortex gliding as a new propulsion concept for UAVs, *Czech Aerospace Proceedings*, 2/2013, 14-16.
[8] Iversen, J. D. 1976. Correlation of Turbulent Trailing Vortex Decay Data. Iowa State University, 23 p.
[9] Bhagwat, M. J., Leishman, J. G. 2002. Generalized Viscous Vortex Model for Application to Free-Vortex Wake and Aeroacoustics Calculations. In *Annual Forum Proceedings-American Helicopter Society*, 2042-2057.
[10] Holzäpfel, F. 2003. Analysis of wake vortex decay mechanisms in the atmosphere. *Aerospace Science and Technology*, 7/2003, 263-275.
[11] Holzäpfel, F. 2003. Probabilistic Two-Phase Wake Vortex Decay and Transport Model. *Journal of Aircraft*, Vol. 40, No. 2, 323-331.
[12] Ahmad, N. N. et al. 2014. Review of Idealized Aircraft Wake Vortex Models, *AIAA paper*.
[13] Delisi, D. P. et al. 2003. Aircraft wake vortex core size measurements. *AIAA Paper*, 3811: 1-9.
[14] Kóňa, M. 2015. Aerodynamic Design of Transonic Glider. Master thesis, Brno University of Technology.
[15] Roskam J. 1990. Airplane Design VI: Preliminary Calculation of Aerodynamic, Thrust and Power Characteristics. Kansas: Roskam Aviation and Engineering Corp., 550 s.
[16] Whitcomb, R. T. 1952. A Study of the Zero-lift Drag-rise Characteristics of Wing-body Combinations Near the Speed of Sound.
[17] Lockwood, V. E., Fikes, J. E. 1952. Control Characteristics at transonic speeds of a linked flap and spoiler on a tapered 45° sweptback wing of aspect ratio 3. NACA RM L52D25.